Analysis of a Helicopter Main Gearbox by means of Numerical Modelling approach

M. Fossati, A. Manes, C. Sbarufatti, M. Giglio*
Politecnico di Milano - Dipartimento di Meccanica, Via Giuseppe La Masa, 1, 20156 Milano, Italy
*- * corresponding author: marco.giglio@polimi.it*

ABSTRACT

The main Gear Box is one of the most critical component of a helicopter drivetrain: high torque and high torque redaction ratio are involved in a lightweight box, including a complex system of gears, bearings and shafts. One of the interesting parameters of the investigation of this complex assembly is the evaluation of the displacements under loads of the gears: this analysis is judged as necessary and meaningful for a prediction of the geometric profile modifications thus saving cost and time with respect to an investigation by means of experimental measurements.
The purpose of this work is therefore to describe the modelling approach of a complex Main Gear Box of an actual helicopter using a FE method approach. Even if the gearbox is a very complex assembly of several components, the aim is to reduce the complexity in the characterization of all the parts, ensuring confidence and likeliness in the results.

1. INTRODUCTION

The exploitation of a modern approach, such as Finite Element Analysis, is herein shown highlighting the indisputable advantages. However, the complexity of the analyses requires a complex validation procedure and a deep insight in the assessment of the possible uncertainty in the result.
To achieve this, each sub system (single bearings and then bearings coupled with shafts) of the gearbox is simulated separately (as a sort of sub model) and the macroscopic behaviour is then transmitted/inserted into the main and comprehensive model of the whole main gearbox. The evaluation of the displacements of the shafts under the workloads of the gears is then assessed: such analysis is judged as necessary and meaningful for a prediction by analyses of the gears and shafts displacements, allowing the application of the geometric profile modifications. In more detail, the first step of this activity is to obtain a simple method to model the gearbox bearings, in order to introduce their equivalent stiffness into the general FE model of the whole main gearbox, see Fig 1. Bearings are modelled using FEM techniques with a commercial Finite Elements software and the stiffness obtained are compared with the results from the commercial software available (Jones, [1]). The second step consists in the introduction of the baring sub-systems simulated and calibrated in the gearbox case. The case is modelled with shell elements while the other parts (gears and shafts) are modelled using solid elements. Bearings are therefore simulated with FE, previously calibrated and substituted with non-linear springs (something missing?), while gears are simulated applying special equations between the displacement of the coincident nodes of two gears in contact, laying on the primitive surface of both. Simulation were performed by means of a static, standard type, and were computed using ABAQUS solver.
It's worth to mention that such an approach allows not only the application of service load but also for a feasible and safe assessment of the system in critical conditions, for instance in case of engine failure. Results are presented in terms of displacements with focus on the nodes belonging to the main central body of the Main gearbox laying on the shaft's mean axes.

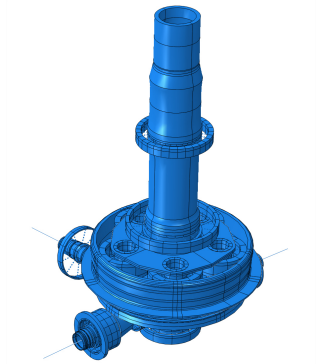

Figure 1 – helicopter gear box

2. WORK OVERVIEW

A method to model the gearbox of a helicopter rotor transmission was developed and herein reported. In fact, the gear box model was derived from a detailed FE model of the gearbox whereas the simplicity regards the type of simulation performed (standard static, instead of a more complex explicit dynamic), and the way the bearings were simulated. The bearings were modelled using FEM techniques with Abaqus software and the stiffness obtained are compared with the results from available commercial software (Jones, [1]). Finally, the results of the gears displacement under load are compared to the analytical solution and to the results provided using the manufacturer's home-made methodologies in order to verify the reliability and efficiency of their methods, which are simplified but considered reliable. For the proceeding, the paper is divided into the following main topics

- Bearing analysis, comparison between the FE and the results obtained from the commercial software results and the definition of the best way to simulate the bearing behaviour (with all its properties, stiffness and load capacity) in the Main GearBox (MGB) complete model.
- Description of the complete MGB FE model with details of the techniques used for the simulation of gears, cases and all their interactions.
- Main results coming from the analysis.

3. BEARINGS DESCRIPTION

For the definition of the methodological approach to be followed for obtaining a FE model as reliable as possible, attention was first focused on the bearings mounted on the pinion shaft (see Figure 2). The main results from this analysis are applicable without any restrictions to all the other bearings mounted in the MGB.

The bearings analysed consists of two configurations: ball bearings (angular contact and four point contacts types) and cylindrical roller bearings; these bearings are mounted on the pinion shaft contained in the transmission.

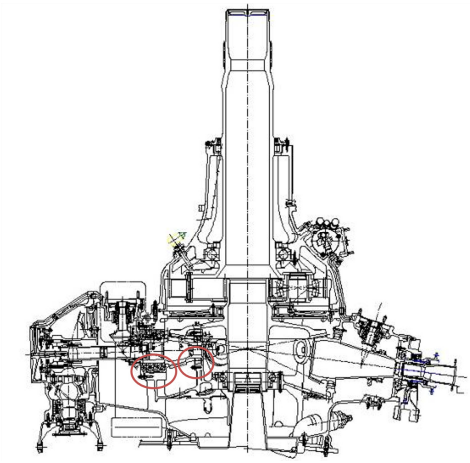

Figure 2 – Load-displacement points from Jones' software for axially loaded ball bearing

As a guide line, the results obtained from the Jones' software for the simulation of the bearing-shafts system was used. This software, based on an analytical approach of a bearings-shaft system, requires the shaft (considered rigid) and the bearings geometry as input and, after loading the system with a specific set of forces, the software returns the reaction forces and displacements of the bearings and the stiffness under the applied load. With a complete set of loads the stiffness curves can be defined by plotting the reaction forces vs the displacements for all the bearings, with an acceptable dispersion. The runs were obtained with different engine power outputs and the loads applied on the shaft in the gear tooth contact zone for each run are summarized in Table 1

Table 1: tab

POWER [HP]	Axial force [N]	Radial force [N]	Tangential force [N]
Stage 6	29270	14064	-46687
Stage 5	23108	11103	-36858
Stage 4	18486	8882	-29487
Stage 3	15097	7254	-24081
Stage 2	10013	4811	-15972
Stage 1	7703	3701	-12286

In the specific geometry considered, the shaft was mounted on three compacted ball bearings and a roller bearing. The roller bearing can handle only the radial load, while the ball bearings can handle both the radial and the axial load. The bearings represent the only joint system between the shaft and the external gearbox and therefore all the reaction forces must pass through them. The zone of contact between the teeth of the two gears was considered as the zone of load application. Finally, in the real system, the final part of the shaft on the turbine side is not free to move, whereas in the simulation carried out this part is considered free as in the Jones' analysis.

The three stiffness curves from the Jones' data output, two for the ball bearings (axial and radial) and curve for the roller bearing (radial) can be reconstructed. Due to the non-linearity of the problem, the curves force-displacement for each roller and ball bearing present a slight but not perfectly linear behaviour.
In the following graphs (Figure 3, Figure 4 and Figure 5), the values obtained from the Jones' software (reaction forces versus displacements) are shown.

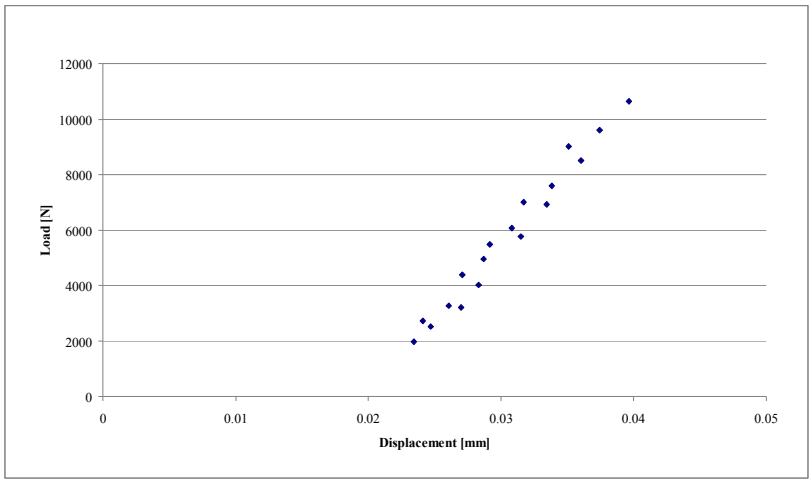

Figure 3 – Load-displacement points from the Jones' software for axially loaded ball bearings

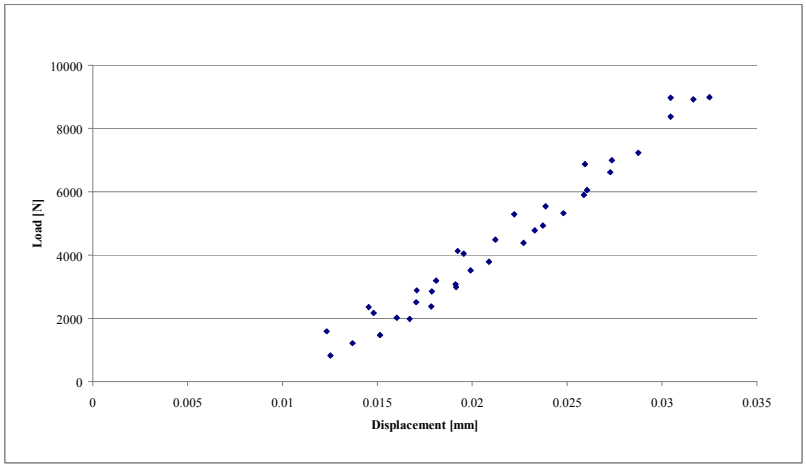

Figure 4 – Load-displacement points from the Jones' software for radial loaded ball bearings

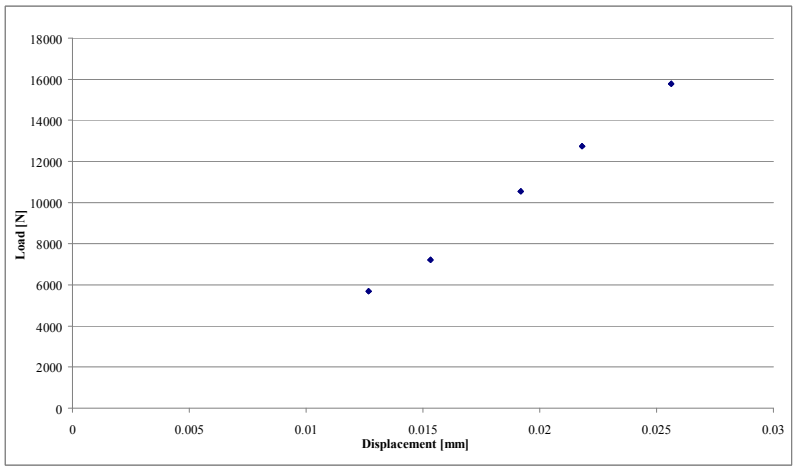

Figure 5 - Load-displacement points from Jones' software for radial loaded roller bearings

4. FE BEARINGS MODEL

For all the simulations, only a portion of the bearing, containing a single rolling element (ball or roller) and a relative portion of the inner and outer rings, was modelled. The stiffness curves obtained by the simulation were then used to calculate the stiffness off the whole bearing, considering its geometry (number of balls and bearing radius), in order to compare the stiffness data with the stiffness curves obtained by the Jones' data output. In a second step, the equivalent

stiffness obtained for this portion of the bearing was introduced directly in the FE model of the whole gear box, in correspondence of the position of the single rolling element; this methodology permits the simulation of the general behaviour of the bearing starting from the model of a single roller part reducing the complexity of the analyses.

4.1 Angular contact, four-point contact ball bearing and Cylindrical roller bearing

All kinds of bearings were modelled using ABAQUS CAE: angular ball bearings, angular roller bearing geometry and mesh are showed in Figure 6. Mesh were generated using Standard Hexaedral, 8-node linear brick, reduced integration with hourglass control, elements.

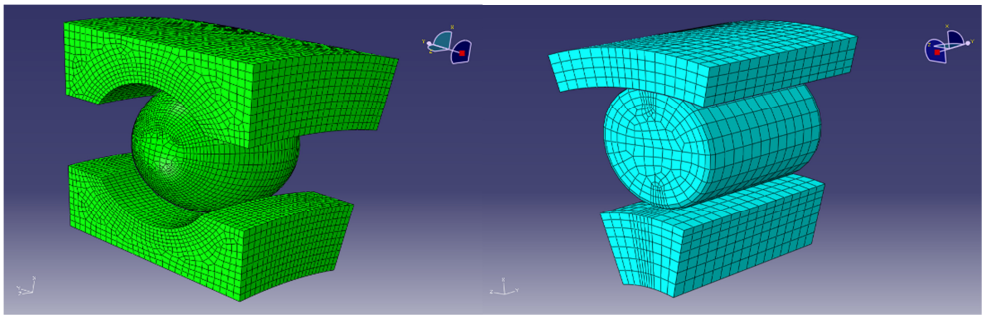

Figure 6 - Single ball and roll bearings geometry and mesh

The interactions among the ball and the rings were described as a mechanical contact and are “normal” and “tangential” types, with an imposed friction coefficient equal to 0.05 that does not modify the results but stabilizes the simulations.
Boundary conditions were imposed to permit the application of only axial and radial assigned displacements. In particular, the external surface of the outer ring was fixed, while the imposed displacements were applied on the internal surface of the inner ring (in radial direction for the radial stiffness evaluation, and in axial direction for the axial stiffness).

5. NUMERICAL ANALYSIS FOR MODEL CALIBRATION

The analyses performed were carried out to obtain a stiffness model able to be introduced in the general model of transmission, with a reduction of the number of elements and nodes involved but with the same reliability of the results. The stiffness obtained for the full bearing, modelled as described above, were compared with the stiffness obtained with the Jones’ software, obtaining very good agreement. However, a more profound analysis was required to consider the effect of the preload on the numerically calculated stiffness. Subsequently further analyses to evaluate the distribution of the reaction forces in a hyperstatic system as the pinion shaft studied were performed. The models considered were gradually deepened, starting with a simple analytical rigid model, then considering a deformable shaft model, and ultimately modelling the full shaft with a FE approach. In all of the models, the bearing stiffness introduced were obtained from the Jones’ software (the stiffness evaluated with the FE models were in all cases very close to these values), in order to compare the reaction results with the Jones’ output with the same initial conditions.

5.1 Single bearing FE model calibration

The following section includes the results of the models run; models differ for mesh density and element type. The first analysis was used to calibrate the FE model versus the data obtained from the Jones' data output, considering an equivalent bearing. The calibration results are shown for axial and radial stiffness (ball bearing) and for radial stiffness only (roll bearing)

5.1.1 Axial stiffness for ball bearing

As shown in *Figure* 7, the FE results present good agreement, compared with the Jones' curve, if a little preload (equivalent to a 0.005 mm displacement imposed) is considered (yellow curve vs. red curve).
A sensitivity analysis on the mesh dimension and the element type was carried out.
As visible in *Figure* 7, a medium density mesh results in a different behaviour, and a more detailed mesh was thus required (selected mesh) to achieve better agreement with the analytical results.

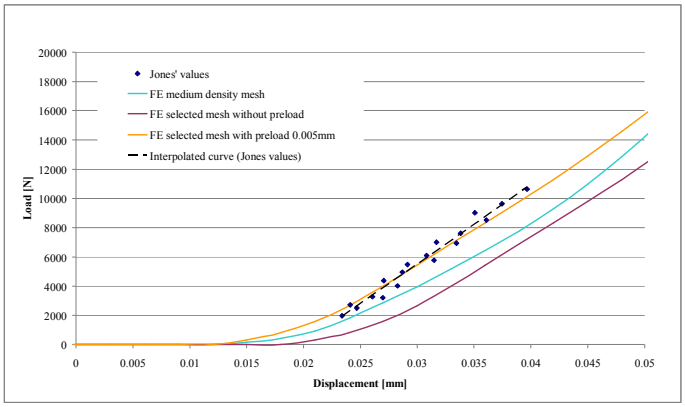

Figure 7 - *Results of mesh optimization and preload on axial loaded ball bearing*

Considering the element type, linear elements were preferred to quadratic ones to obtain reasonable computing time and a more robust resolution of the contacts.

5.1.2 Radial stiffness for ball bearing

The radial stiffness evaluation, does not require the preload application, and the bearing stiffness behaviour stands in good agreement with the analytical results (Figure 8) considering the mesh identified as the best one from the previous optimization.

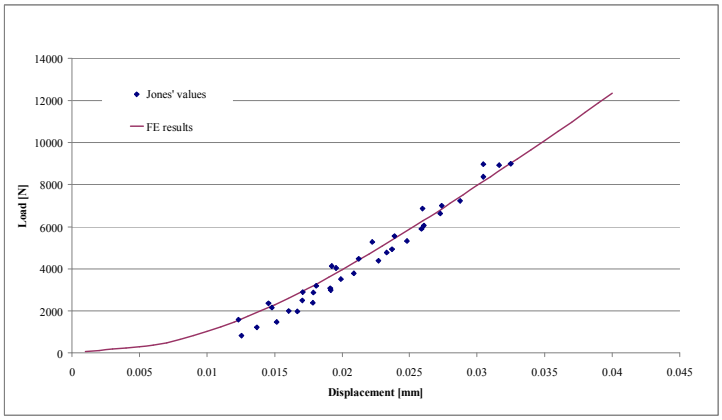

Figure 8 - *Radial loaded ball bearing load-displacement curve*

5.1.3 Radial stiffness for cylindrical roller bearing

Also for the roller bearing behaviour, a little preload (equivalent to a 0.005 mm displacement imposed) was considered to obtain good agreement with the Jones' curve with regards to the radial stiffness (*Figure* 9).
The element type and the mesh refinement were taken from the previous analysis.

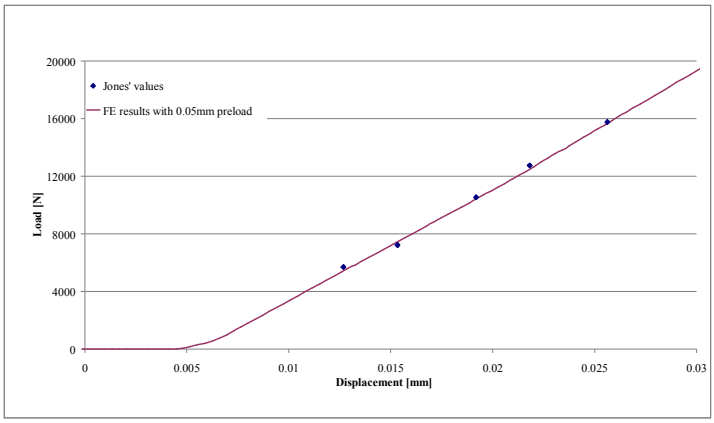

Figure 9 - Radial loaded roller bearing load-displacement curve

The next step consists evaluation of the reaction forces. Forces instead of displacements were proposed according to the manufacturer. Despite this, as the stiffness curves of the bearings are almost comparable thanks to the calibration of the models, the results of the comparisons can be translated to the displacement domain without the loss of the general meaning of the conclusions. The evaluation of the reaction forces was obtained comparing different approaches with different levels of complexity.

6. Monodimensional shaft equipped with bearings

The initial approaches considered a shaft modelled with a single beam, rigid in the first model and subsequently deformable; this method permits the control of the final result, which is linked to the initial values by means a progressive modification of the results obtained.
This step by step approach is considered more simple and reliable, with the best control of the last model chosen.

6.1 Analytical model with a mono-dimensional rigid beam

The first simple model is an analytical model, with a rigid beam used instead of the shaft and a set of grounded springs simulating the bearing. The stiffness of all the springs was obtained from the Jones' results using a Stage 9 engine power output and is reported in *Table* II.

STIFFNESS							
BEARING	BEARING	Axial position	K_X X direction	K_Y Y direction	K_Z Z direction	$K_{Y,rot}$ Y direction	$K_{Z,rot}$ Z direction
NUMBER	TYPE	[mm]	[N/mm]	[N/mm]	[N/mm]	[Nmm/rad]	[Nmm/rad]
1	BALL	103.0	2.6573E+05	2.7163E+05	2.9415E+05	3.1835E+08	3.5883E+08
2	BALL	80.0	2.5148E+05	2.7591E+05	2.4377E+05	2.7870E+08	3.6971E+08
3	BALL	57.0	2.4829E+05	2.8735E+05	2.0892E+05	2.5941E+08	3.8996E+08
4	ROLLER	-62.3	0.0000E+00	6.5267E+05	3.2857E+05	4.7944E+06	1.1782E+07

Table II *– Stiffness of the bearing from Jones' analysis*

The X axes in the coordinate system were directed along the system shaft's line, while the Y-Z axes were in the bearing plane, normal to the shaft, as well.
The loads at a Stage 6 engine power output were used to test the shaft.

6.2 FE model with mono-dimensional deformable beam

In the second approach, a shaft modelled with FE beam elements joined to the ground with a spring system was used, identical to the one used in the rigid approach explained below.
In this case, the shaft mounted on the bearings was simulated with mono-dimensional beam elements, using the linear and angular stiffness from the Jones' software.

The transversal sections used for the beam elements were obtained from a simplified model in which every portion of the shaft is a hollow cylinder; the conical part was considered with its average diameter.
In *Figure* 10 a plot of the beam element model, with loads, torques, longitudinal and angular stiffness as from used for the Jones' simulations [1] is reported.

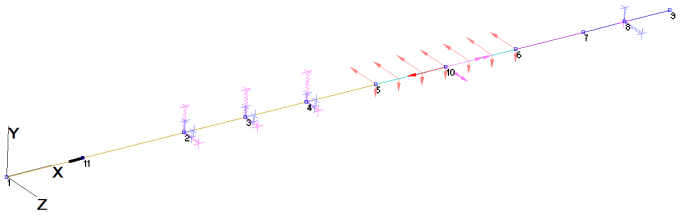

Figure 10 - *Beam shaft and springs system*

7. Three-dimensional shaft with bearings

A more accurate analysis was performed with a three-dimensional FE model of the shaft.
The elements used are 8 nodes linear elements with a reduced integration. The geometry was provided by the manufacturer. To compare the results with the previous ones, two models were made: a model with an equivalent linear set of springs for each bearing ring, obtained from the Jones' output, and a model with a set of non-linear springs, obtained from the previous FE model of the bearings, for each ball and roller bearing.

7.1 FE model with linear springs from the Jones' output

In the first model, the ground links were made in the same way as the previous FE simulation, with a set of grounded springs (one for each bearing ring) with a fixed stiffness. The shaft mounted on the bearings was then modelled with hexahedral elements, using linear and angular stiffness from the Jones' software (see *Table* II). The materials were equivalent to the ones used for the simulation of the bearing (standard steel). The geometry of the shaft with the mesh is shown in *Figure* 11. The displacements of each section of the beam (middle section is taken), in which each bearing acts, were governed by a reference point, located on the axes line of the shaft, and connected to the rest of the bearing' sections by kinematic couplings.

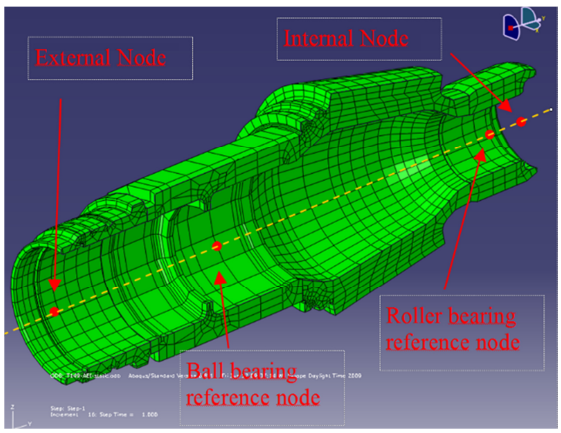

Figure 11 - *Pinion gear 8 nodes elements mesh and reference control nodes*

7.2 Detailed FE model with FE stiffness model for bearings

In the last and most detailed model, each ball and roller in bearings were simulated with a set of non-linear springs for each bearing. The springs were modelled with the force-displacement curve previously obtained in the FE model of the bearings (see Section 5).
The geometry used for the FE model of the shaft was derived from the model file from the manufacturer, and it is shown in *Figure* 12. In this model, each ball/roller was described as a spring with radial/axial stiffness, as the results from the previous FE models.

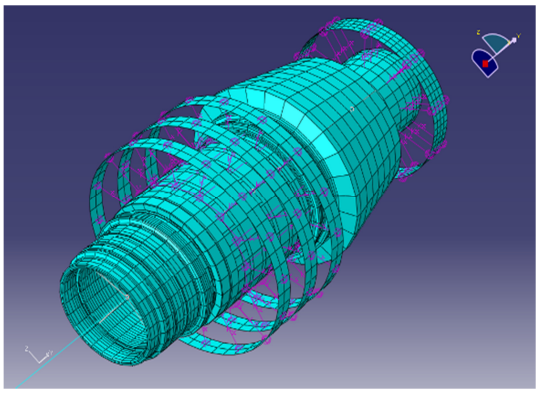

Figure 12 - *Full meshed FE model of the pinion gear with non-linear springs*

8. COMPARISON OF THE RESULTS AND CONCLUSIONS

With regards to the stiffness evaluation of the bearings, the FE model results are in good agreement with the values obtained with the Jones' software. However, a more profound analysis was executed to consider the effect of preloads and meshes on the bearing stiffness: in particular, regarding the axial stiffness, an initial preload could substantially modify the bearing behaviour. The critical evaluation of the effect of the bearing stiffness on the behaviour of the system, linked to the ground by way of the bearings is more complex.

The analyses conducted gave a different scenario regarding the reaction forces, depending on the method used to simulate the shaft behaviour. In the next tables the reaction forces obtained with the different methods are reported. The Analytical (rigid beam) model was not used for the simulation of the axial load [X direction], as well.

BEARING NUMBER	Analytical model, rigid beam, X reaction force [N]	FE 1-D model, deformable beam, X reaction force [N]	FE 3-D model, bearing stiffness from Jones, X reaction force [N]	FE 3-D model, bearing stiffness from FE model, X reaction force [N]	Jones' software, X reaction force [N]
1	Not Run	-9855	-9996	-9438	-10966
2	Not Run	-9569	-9579	-9673	-9591
3	Not Run	-9845	-9694	-10158	-8748
4	Not Run	0	0	0	0
Sum of the reaction forces	Not Run	-29269	-29269	-29269	-29305

Table III *– Reaction forces compared for 1900 HP engine power, X direction*

BEARING NUMBER	Analytical model, rigid beam, Y reaction force [N]	FE 1-D model, deformable beam, Y reaction force [N]	FE 3-D model, bearing stiffness from Jones, Y reaction force [N]	FE 3-D model, bearing stiffness from FE model, Y reaction force [N]	Jones' software, Y reaction force [N]
1	6386	6418	5866	4785	8894
2	7070	8006	8187	7044	8724
3	7970	9859	11311	10297	8653
4	25261	22400	21321	24100	20170
Sum of the reaction forces	46687	46683	46685	46226	46442

Table IV *– Reaction forces compared for 1900 HP engine power, Y direction*

BEARING NUMBER	Analytical model, rigid beam, Z reaction force [N]	FE 1-D model, deformable beam, Z reaction force [N]	FE 3-D model, bearing stiffness from Jones, Z reaction force [N]	FE 3-D model, bearing stiffness from FE model, Z reaction force [N]	Jones' software, Z reaction force [N]
1	6217	6059	6063	4895	9585
2	4453	4835	4813	4981	6749
3	3218	3967	4069	5290	4409
4	176	-798	-883	-1166	-5274
Sum of the reaction forces	14064	14064	14062	14000	15468

Table V – Reaction forces compared for 1900 HP engine power, Z direction

All the results showed a similar trend, however a progressive difference between the results from the analytical rigid model, the FE beam deformable model and the 3-D FE model was apparent.
On the contrary, the results from the Jones' software highlighted a different behaviour, with more evident discrepancies which necessitated another step of analysis and research to understand the origin of the disagreement of the reaction achieved with different methods.
The reason for the existing discrepancies between the outcomes coming from the Jones software and from the analyses carried out using the FE approach, reported in the tables above, can be attributed to the correct definition of the radial, axial and angular stiffness provided by the Jones' output and the ones provided by the FE analysis. The "concept" of stiffness calculated by the Jones' seems different from the typical one defined using the FE approach and normally established by a simple ratio between an applied force and a recorded displacement. In particular, the contents of Paragraphs0 5.1.1 to 5.1.3 demonstrated that a good correlation between the bearing stiffness evaluated using the FE approach and the one calculated using the Jones' output was found. The main problem is to introduce these stiffness values in a global model for the simulation of the complete integration between the items: in the FE approach, the springs simulating of the stiffness was introduced locally, in each section of the shaft in contact with the middle surface of the bearing, however when using the Jones' output different methods were followed. Therefore, the difference found in the different models (in terms of reaction loads in correspondence of the bearings) can only be resolved by approaching more detailed methods of simulation and by calculating the bearings.
Nevertheless, the proposed methodology can be used in the FE global model of the MGB central body because this model aims to estimate the displacements of the gears under applied loads and for this purpose, it is important to have a good correlation between the displacements recorded by FE and the ones estimated using Jones; this assures that the correct deflections of the shaft are applied with a correct estimation of the gears displacements under load, the main topic of this analysis.

9. FULL TRANSMISSION MODEL

The complete model was generated according to the previous approach for the bearings and shaft simulation; the bearing system was finally modelled by a series of wires and non-linear connectors and the stiffness curves of each component were obtained from specific FE models of the single bearing. The shafts were finally connected point to point to the main external body of the transmission (main case and top case) by the bearing system. Each shaft was also connected to each other through a specific equation system in the gear teeth contact zone, forcing the displacements of each contact nodes to move coupled in the gear contact pressure direction. External boundaries were considered connected to ground, whereas the main external body and workloads were considered as introduced moments. The simulation was supposed to be static with large displacements and rotations.

9.1 Model details

The model is composed of a main shaft (mast), driven by a system of five gears that are connected to a fixed ring (in the external part) and to a central gear in the inner (SUN). The inner gear is part of the collector gear at which the two pinions, for power input, and the tail shaft are connected too (*Figure* 13).
The external part of the gear box (*Figure* 14) is composed by a shell part (top case) and a solid part (main case).

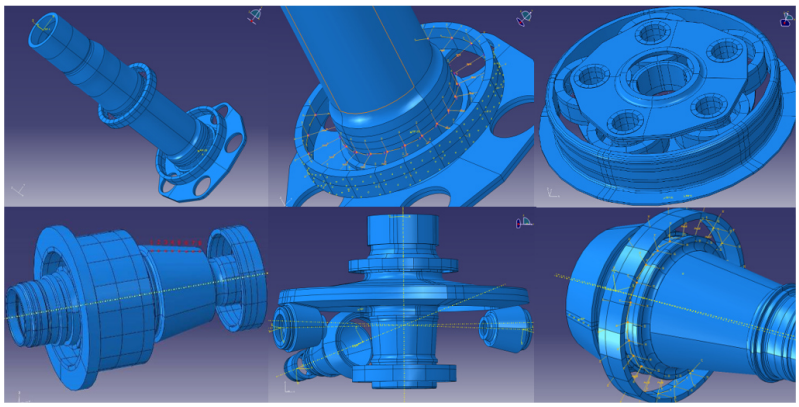

Figure 13 – *Parts and assembly of the transmission*

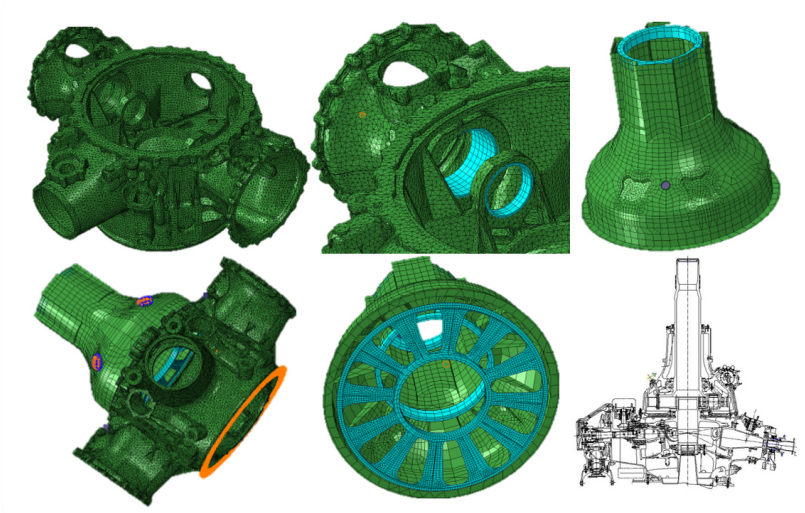

Figure 14 – *Parts and assembly of the gear box shell*

Each connection of the shaft was simulated with the introduction of a series of non-linear springs, as previously explained, whose stiffness was calculated as explained above; whereas the bearings of the gears of the SUN were simulated considering the bearing systems as rigid (in fact, the stiffness of the flanges of the mast, housing the gears, was considered to be far less stiff). The interactions between the gears in the SUN (Figure 16 A) were simulated by connecting a line of nodes (Figure 16 B), coincident for two connected gears and acting on the primitive line, to move radially of the same length but in the opposite direction. Particular importance was dedicated to the pinions (Figure 16 C, with mesh overview, and Figure 16 D, with components and force scheme overview), which were connected to the gear box body by a more complex system of bearings, with respect to what was shown in Paragraph 7.1, involving even the axial behaviour. The axial behaviour of the bearings is crucial in the study of the displacements of the shafts due to the presence of the conical gear connecting them to the collector gear.

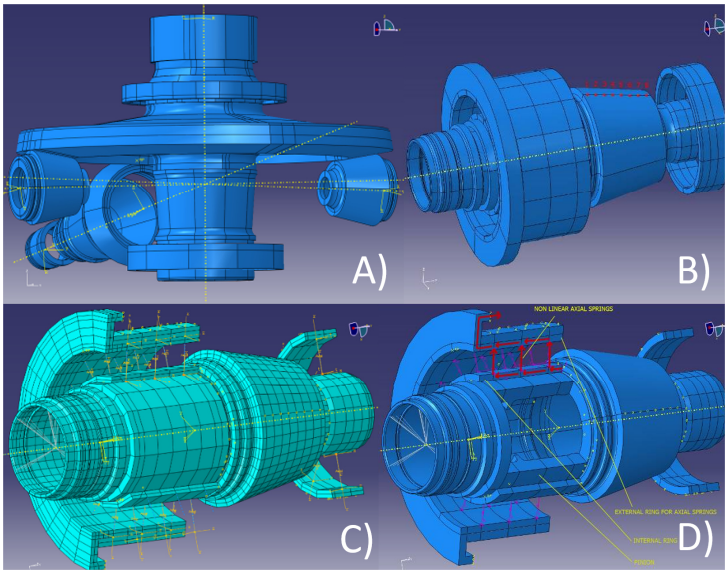

Figure 15 – *Collector Gear equipped with bearings and shafts*

The locking of the rotations of the mast and the application of the real power on the three shafts appeared to be the simplest way to apply moments and displacements. However, due to a reduction ratio of nearly 25 times from the pinion engine to the mast, the rotations should have been increased by nearly 25 times instead of locking the pinions and applying the moment directly on the mast. Finally, ground locks were imposed on the gear box shell in the dedicated locations. Six load cases were tested: Two load cases were performed to analyse normal operative functionality, with a static run and a fatigue run. The other four cases represent a one engine failure scenario, tested for both of the two pinions, in static and in fatigue verification.

10. RESULTS

The results were collected in terms of displacements. In the following, the normalised results of the load case 1 are shown in particular, attention was paid to the displacements of the nodes belonging to the main central body of the MGB, i.e. the left and right pinions, the collector gear and the tail rotor pinion. Details regarding the location of the reference nodes used for the displacements evaluation are shown in Figure 17. The coordinate system, in which the displacements was measured, was made with the U3 direction directed along the main shaft axes, the U2 was directed towards the engagement planes of gear of the shaft.

CONDITION 1 - STATIC (AEO)							
SHAFT'S MEAN AXES NODES DISPLACEMENT, POSITION OF THE NODES							
LEFT PINION COORD SYSTEM		DISPLACEMENTS [mm]			NODE POSITION, GLOBAL COORD [mm]		
LEFT PINION	node	U1	U2	U3	X	Y	Z
external node	2	-0.118	-0.098	-0.102	-0.861	375.566	-128.971
Internal node	25	-0.118	0.114	-0.213	-0.322	140.521	-122.816

LEFT PINION COORD SYSTEM		DISPLACEMENTS [mm]			NODE POSITION, GLOBAL COORD [mm]		
COLLECTOR GEAR	node	U1	U2	U3	X	Y	Z
Upper node	1	-0.104	0.288	0.251	0.000	0.000	-247.918
Lower node	26	-0.068	0.312	-0.048	0.000	0.000	22.937

SHAFT'S MEAN AXES NODES DISPLACEMENT, POSITION OF THE NODES		
RIGHT PINION COORD SYSTEM	DISPLACEMENTS [mm]	NODE POSITION, GLOBAL COORD [mm]

RIGHT PINION	node	U1	U2	U3	X	Y	Z
external node	2	-0.117	-0.097	-0.064	0.861	-375.566	-128.971
Internal node	24	-0.117	0.116	-0.239	0.322	-140.521	-122.816

RIGHT PINION COORD SYSTEM		DISPLACEMENTS [mm]			NODE POSITION, GLOBAL COORD [mm]		
COLLECTOR GEAR	node	U1	U2	U3	X	Y	Z
Upper node	1	0.119	0.283	-0.251	0.000	0.000	-247.918
Lower node	26	0.084	0.308	0.048	0.000	0.000	22.937

SHAFT'S MEAN AXES NODES DISPLACEMENT, POSITION OF THE NODES							
TAIL SHAFT COORD SYSTEM		DISPLACEMENTS [mm]			NODE POSITION, GLOBAL COORD [mm]		
TAIL SHAFT	node	U1	U2	U3	X	Y	Z
external node	4	0.090	0.024	-0.287	-580.994	0.000	-195.625
Internal node	21	0.099	-0.272	0.236	-249.624	0.000	-152.000

TAIL SHAFT COORD SYSTEM		DISPLACEMENTS [mm]			NODE POSITION, GLOBAL COORD [mm]		
COLLECTOR GEAR	node	U1	U2	U3	X	Y	Z
Upper node	1	-0.212	0.316	-0.111	0.000	0.000	-247.918
Lower node	26	0.088	0.301	-0.076	0.000	0.000	22.937

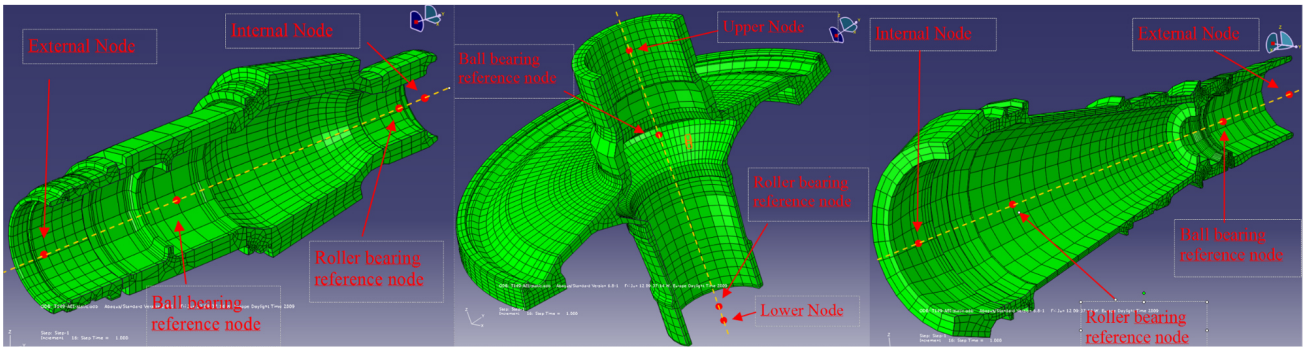

Figure 17 Pinions, Collector Gear and Tail shaft reference points

The displacements read in correspondence of the nodes belonging to the MPC equation and the values recorded in correspondence of the dummy nodes representing the bearings location were compared. The utility of this comparison arises from the necessity to have a confirmation of the reliability of the methodologies used internally in TSD & D for the evaluation of the gear displacements under load. In particular, this comparison has evidenced that the displacements read in correspondence of the MPC equation nodes are mainly due to the bearings seats displacements with negligible weight due to the shaft deformation under load. This assesses the reliability and efficiency of the methodology followed in TSD & D: in particular, the gears load pattern was estimated by evaluating the deformation of the bearings seats without considering the shaft stiffness.

11. CONCLUSIONS

An approach based on FE analysis for the complete simulation of the H/C transmission system was presented in this test report. The first step of the analysis was focused on the definition of a bearing FE model fully representative of the bearing behaviour under load, in terms of stiffness, displacements and reaction forces. Models were developed for both the typical bearing

configurations, the roller and the ball one. The first step was aimed to simulate the single ball; afterwards, the complete 3d model of one ball and the relative seats (another model was developed for the roller type bearing) was generated. The main outcomes of this first analysis were nonlinear stiffness curves, valid for the modelled ball/roller geometry.
A complete bearing ring was modelled replacing each ball with the equivalent nonlinear spring obtained from the 3d FE model; the stiffness curves of the whole bearing system were compared with the Jones data (for the ball and the roller bearing). Finally, in order to verify the nonlinear-spring representation of the bearings in a more complex case, a comparison with the Jones software has been carried out. A shaft with a series of roller and ball bearings was simulated with a mathematical approach, an ABAQUS approach, and the Jones' software. All the analyses mentioned above were performed under the same load conditions, thus allowing the comparison of the results
The results were:

- A good correlation between the stiffness evaluated by FE and the ones estimated using the Jones software was found, both for the roller and for the ball bearing.
- A comparison between the bearings displacements read using the FE model and the ones recorded by Jones was performed, evidencing that similar values were obtained, thus confirming that the shaft deformation evaluated by FE is similar to the one calculated by Jones.
- As a last step, the reaction forces were checked: the values recorded in the FE analysis differed from the ones calculated by the Jones' software. The difference was found not only in the load values but also in the load distribution on the bearing.

The similar stiffness values, together with the similar displacements read by FE and by the Jones software assure that the FE model generated for the bearing simulation is reliable for the estimation of the gear displacements under load, thus leading to the conclusion that the bearing FE model is usable without any restrictions in the complete MGB FE model providing good results in terms of gear displacements, the parameters under analysis. The second part of the activity was focused on the generation of the complete 3d model of the transmission system.
In conclusion, a model was generated with good results. This model can be used to evaluate particular load conditions and different gears contact behaviour between the collector and the other shafts. With a sub-structure system of the gears contact, it should be possible to generate a zone of real contact between, for example, the collector and the pinion, generating solid models of the zone of contact in separate files that interact with the main simulation. A modification of the geometry in the contact solid file will produce a modification of the behaviour of the main simulation and can be useful in the evaluation of the best geometry configuration.

References

[1] A.B. Jones “A general theory for elastically constrained ball and radial roller bearings under arbitrary load and speed conditions”, ASME publication N. 59-LUB-10, 1960.